

Fractal Structure of Shortest Paths in Native Proteins and Determination of Residues on a Given Shortest Path

Burak Erman

Department of Chemical and Biological Engineering, Koc University, Istanbul, Turkey

email: berman@ku.edu.tr

Fractal structure of shortest paths depends strongly on interresidue interaction cutoff distance. The dimensionality of shortest paths is calculated as a function of interaction cutoff distance. Shortest paths are self similar with a fractal dimension of 1.12 ± 0.03 when calculated with step lengths larger than 6.8 \AA . Paths are multifractal below 6.8 \AA . The number of steps to traverse a shortest path is a discontinuous function of cutoff size at short cutoff values, showing abrupt decreases to smaller values as cutoff distance increases. As information progresses along the direction of a shortest path a large set of residues are affected because they are interacting neighbors to the residues of the shortest path. Thus, several residues are involved diffusively in information transport which may be identified with the present model. An algorithm is introduced to determine the residues of a given shortest path. The shortest path residues are the highly visited residues during information transport. These paths are shown to lie on the high entropy landscape of the protein where entropy is taken to increase with abundance of visits to nodes during signal transport.

Introduction

Flow of energy or information in general, from one point to another in native proteins depends on the spatial arrangement of amino acid residues. There is a close relationship between fractal structure and information transport in proteins which has been studied by several authors and reviewed by Leitner ¹. For a dense, homogeneous system, energy may flow in three dimensions which is characterized by the spectral dimension of 3 obtained from the celebrated Debye density of states expression. For such media, the mass dimension which is the Euler dimension is also 3. The three dimensional structures of proteins are neither dense nor homogeneous, and consequently the dimensionality for the propagation of energy, i.e., the spectral dimension, and the mass fractal dimension both deviate from 3. The value is around 1.7 for the spectral dimension ²⁻⁴ and 2.5 for mass fractal dimension ⁵. The loss in spectral dimension results from the fact that not every path is allowed for a signal to proceed from one point to the other in the protein. Similarly, the loss in mass fractal dimension is because one can only travel in the protein from atom to atom, and the problem

is similar to random walk on lattices^{1,6}. However, in contrast to random walk, information flow is anisotropic in proteins and the possible routes in the protein are constrained by the presence of irregularities in mass density. Moreover, the specific structure of a protein evolved for fulfilling and optimizing a specific function is expected to impose constraints on flow of energy, such as going over the shortest path, shortest time, least resistance, through highly visited nodes, or combinations of these. In allosteric information transport, for example, it is plausible to expect flow along the shortest path in the fractal architecture for which the transit time, quality, robustness, and noise-independence of signal transmission should be of major concern. Imposing motion to follow shortest paths rather than diffuse over space reduces the dimensionality significantly to values between the upper limit of 3 and the lower limit of 1, The latter is the dimension of the shortest path in homogeneous Euclidean space. In this paper, based on residue contact maps of proteins, we analyze the physics of shortest paths, their fractal dimensions, and present a computational algorithm for determining the residues on a given shortest path.

Among several possible paths between two points i and j in a protein, there exists one or a small number of paths that carry the information from i to j in the smallest number of steps for a given step size. The step size depends basically on the range of interactions in the structure, the fractal structure that determines the interacting neighbors, and the characteristic length scale of the perturbation. We emphasize the dependence of interactions on step size throughout the paper. In the following section, we give a precise definition of shortest path between two points in proteins and outline the calculation of shortest path dimension and the Hausdorff dimension. The identification of residues that lie on a given path is an important problem since it is usually the desire to understand their behavior and manipulate them. We outline a method for determining the residues that lie on a given shortest path. We also show that the path residues are the highly visited residues among the larger set of residues that are indirectly perturbed in the neighborhood as signal propagates. This has a thermodynamic significance indicating that the shortest path among others is a low entropy barrier path.

The characteristic packing of helix-beta-coil structures exhibits an unusual dependence on step size. The number of steps to span a path is obviously very large for very small step sizes. The decrease in the number of steps with increasing step size is not continuous, however. An infinitesimal increase in step size may result in a sudden drop in the number of steps. This behavior is representative of an abrupt change of regime which may have significance when small wavelength perturbations propagate in the fractal structure of the protein. For step sizes in the order of the first coordination shell radius and larger, shortest paths have dimensionality of around 1.1, surprisingly close to that of Euclidean paths. Our calculations are based on a large number of paths from several proteins. All calculated entities show the same features as outlined in more detail below.

Methods and Materials

Unlike dense homogeneous continuous media, a protein is discontinuous, locally anisotropic and inhomogeneous⁷ in which signal travels on a contact map in steps. A signal can go from a point to its neighboring point in one step if the two points are interacting directly, i.e., if they are ‘connected’ in the language of graph theory. The connection is defined in terms of an interaction radius whose magnitude is kept as a variable in this analysis. Its choice directly affects the entries of the contact matrix and the physics based on the contact matrix. The interactions may depend on the characteristic wavelength of the signal. High frequency perturbations may activate the interactions of nearby atoms whereas low frequency ones may activate distant neighbors.

The shortest interaction path between two points i and j is obtained when the signal goes from i to j in a minimum of n steps of a given step size. At lengthscales of the order of first coordination shell and below, which are the relevant scales for signal transmission, native proteins are not self-similar objects (See below). A multitude of fractal dimensions are active at these scales and their detailed understanding is needed for predicting and controlling protein function, most importantly for determining allosteric pathways and modifying them. For long wavelength perturbations, a single fractal dimension is obtained for these paths, which is determined basically by the contact topology and is otherwise independent of the detailed three dimensional structures of the proteins. Fractal structure of native proteins has been addressed in several papers^{1, 5, 6, 8-14}. Here, we focus on fractal properties of shortest interaction paths in proteins, and in this respect it is a new addition to the existing knowledge on protein structure and function. We keep the term ‘interaction’ general, which may result from any source of perturbing effect.

We let r_c denote the interaction cutoff radius and treat it as variable in order to understand the dependence of fractal behavior on different lengthscales of interaction. A perturbation with a wavelength less than r_c generates interactions within a sphere of radius r_c . The ij 'th element of the contact matrix C is 1 if the points i and j are within r_c and zero otherwise. We adopt the alpha carbon representation of the protein. Two alpha carbons do not interact directly if they are at a distance larger than r_c . Below, we obtain the fractal dimension of shortest interaction paths in proteins as a function of r_c .

Fractal Dimension of Shortest Interaction paths: The emphasis is on finding the shortest path among a multitude of paths between two points on the protein. Starting from a residue i , one can go to residue j following a path of interacting residues. We are interested in finding a path traversed with a minimum number of steps, each step being defined as hopping from one point to its interacting neighbor. One can go from i to j in k steps in m different ways. In terms of the contact matrix, $m = [C^k]_{ij}$, i.e., the ij 'th element of the k 'th power of C . The minimum number of steps to go from i to j , k_{\min} , is obtained when $[C^{(k-1)}]_{ij} = 0$ and $[C^k]_{ij} \neq 0$ ¹⁵. The minimum number of steps k_{\min} will be a function of r_c . In an Euclidean dense homogeneous uniform object, the path will be a

straight line from i to j , and we will have $r_{ij} = k_{ij,\min} r_c$, where r_{ij} is the Euclidean distance between i and j . For the protein, this will not hold due to fractal morphology. The minimum number of steps in going from i to j will be expressed in terms of a power law: $r_{ij}^D = A k_{ij,\min} r_c$, where D is the fractal dimension and A is the constant of proportionality of dimension $D-1$. For long paths, we show in the Supplementary Material Section 1 that D is written as

$$D = \frac{\log(k_{ij,\min} r_c)}{\log(r_{ij})} \quad (1)$$

This definition of dimension will strictly hold for a large system and will read as $D = \lim_{\frac{r_{ij}}{r_c} \rightarrow \infty} \frac{\log(k_{ij,\min} r_c)}{\log(r_{ij})}$. For proteins with finite dimensions, Eq. 1 serves as a good approximation to dimension as shown below.

The Hausdorff dimension D_H of fractal paths is obtained from the expression ¹⁶

$$D_H = \lim_{k \rightarrow \infty} \frac{\log(N_k)}{\log(1/r_k)} \quad (2)$$

where the path is partitioned into N_k segments of length r_k each. For the shortest path, we identify the length of segments r_k with the cutoff distance r_c and N_k with $k_{ij,\min}$.

Determining the residues along the shortest path:

Given the end residues, $i_{\{i\}}(0)$ and $i_{\{i\}}(N)$. The numbers in parenthesis give the step number along the directed walk from the starting to the ending residue and the subscript indices in braces give the set of residues that are neighbors to the residues involved in the previous step. Thus, the set $\{j\}$ at an intermediate point will contain more than one residue. The residues involved at each step are candidate residues that contain the residue of the shortest path which will be identified during backtracking (See below). In the first step, starting from $i_{\{i\}}(0)$ we find the set of residues $i_{\{j\}}(1)$ that can be accessed from $i_{\{i\}}(0)$. The residues $i_{\{j\}}(k)$ are accessed from the residues of the previous step $i_{\{j\}}(k-1)$. Residue j at the k th step will be accessed by $v_{\{j\}}(k)$ different paths from residues of the previous step. The set of residues involved in going from $i_{\{i\}}(0)$ to $i_{\{i\}}(N)$ is $\{i_{\{i\}}(0), i_{\{j\}}(1), i_{\{j\}}(2), \dots, i_{\{j\}}(k-1), i_{\{j\}}(N)\}$ and the number of arrivals to the residues from previous

paths during the forward trip is $\{1_{\{j\}}(1), v_{\{j\}}(2), \dots, v_{\{j\}}(k-1), v_{\{j\}}(N)\}$. The residues of the shortest path, $\{i_0, i_1, i_2, \dots, i_{k-1}, i_k, \dots, i_N\}$ are obtained by backtracking, starting from N and going step by step to 1. When the residue at step k is identified in this way, the residue at step k-1 is determined from the list of residues that are adjacent to residue k, already determined in the previous step. This process of backtracking may lead to more than one shortest path, all of which may be identified individually by the backtracking method. Sample calculations for the path from LYS132 to ASP98 in 1GPW.pdb are presented in Supplementary Material Section 2.

Entropy in signal transport:

Identification of the shortest path residues also leads to the set $\{v_1, v_2, \dots, v_{k-1}, v_k, \dots, v_N\}$ identifying the number of visits to each residue along forward tracking, i.e., along the traveling direction of information. The frequency of visits to the i 'th residue is written as $f_i = \frac{v_i}{\sum v_i}$ where the

sum in the denominator for all visits to all residues involved in forward tracking. The denominator here is representative of the space available to the forward tracking process. The entropy of information transport over the shortest path may then be defined as $S/k = -\sum f_i \log f_i$ where the sum is over the residues of the shortest path. According to this definition, the total entropy of transport using all paths is the sum of entropies of transport through individual paths. It is plausible that a signal will choose high entropy paths in the absence of imposed additional constraints. It should be added that since the shortest path is directional, i.e., the nodes visited in going along the forward and reverse directions are different, the entropies of signal transport in the forward and reverse directions will be different.

Results

Values of D from Eq. 1 are calculated for 150 paths from ten proteins from the Protein Data Bank (3K8Y, 1SHJ, 4FHB, 2V20, 2V1Z, 3PGF, 4EZF, 4H7U, 1GPW, 4N4J) and presented in Figure 1 as a function of r_c . These proteins are known to participate in allosteric activity. For each of the 10 proteins 15 paths are chosen such that $r_{ij} \geq 40 \text{ \AA}$ for each path, summing up to 150 paths in total. The filled circles represent the average of the 150 paths. Unfilled circles represent the averages for each of the 15 paths from each protein.

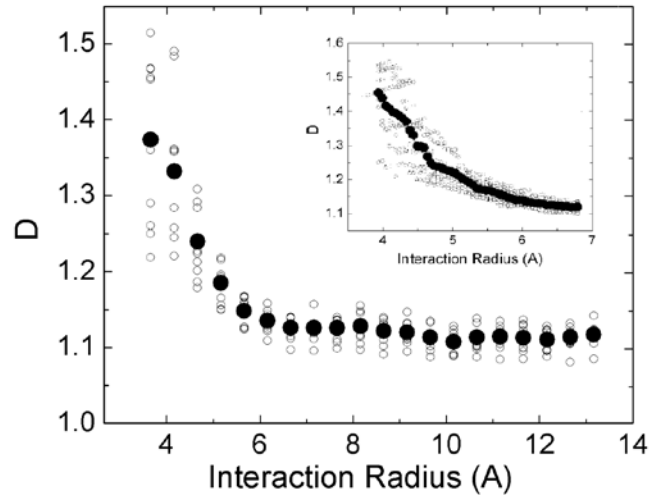


FIG 1. Fractal dimensions of interaction paths in proteins as a function of interaction cutoff radius. Filled circles show averages for 150 different paths from 10 proteins. Empty circles show averages for 15 paths from each protein. The lowest bond percolation limit is ca. 3.8 Å below which a path does not exist in the alpha carbon representation. Inset shows details at smaller interaction radii.

Generally, fractal objects are characterized by a single number¹⁶ which is true for self similar objects. Proteins are not self similar at every length scale as can be seen from the figure. Above lengthscales of $r_c \approx 6.8$ Å, interaction paths have single fractal dimension of $D = 1.12 \pm 0.03$ obtained from Figure 1. However, below $r_c \approx 6.8$ Å, the protein is multifractal; exhibiting different values of D for different interaction radii, starting from average values of $D = 1.4$ at the percolation threshold of ca. 3.8 Å. A closer look to the multifractal range, the inset in Figure 1, surprisingly shows that there is a fractal transition at a length scale slightly below 4.5 Å. At lengthscales below this limit, the system traverses the path between points i and j in a large number of steps, but at the transition point, this number exhibits a jump to lower values. This behavior is observed for all of the ten proteins studied. The magnitude of the drop and the corresponding interaction radius differ from protein to protein, however. This transition is due to the sharp decrease in the number of steps in going from the initial to the final point on the path as the step length increases. This is shown in Figure 2 for the protein 1GPW.pdb for the known allosteric path^{17,18} from LYS132 to ASP98 (See Supplementary Material for more details). LYS 132 is at the allosteric site to which a ligand binds and the effect of binding is transmitted to ASP98 which is 29 Å away. In fact there is more than one sharp drop, closely spaced in the range 4 to 5 Å. This is also true for all the other proteins studied.

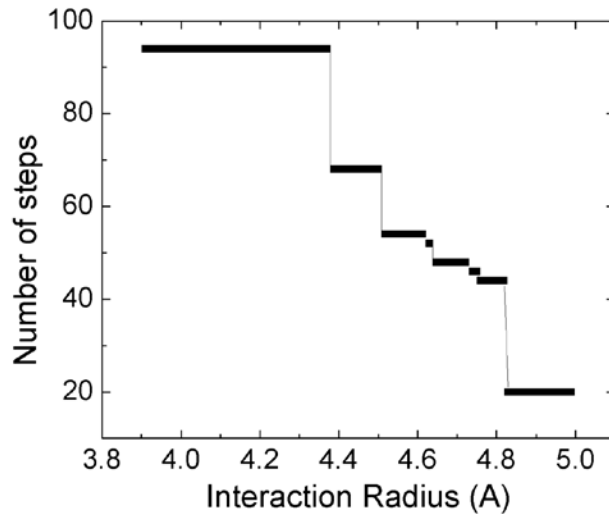


FIG 2. Discontinuities of number of steps at small wavelengths for 1GPW.pdb for the shortest path from residue LYS132 to ASP98.

In Figure 3, we present results of calculations of the Hausdorff dimension calculated using Eq. 2 for 150 paths from the set of ten proteins. The straight line is the least squares fit to the data points. Its slope, which approximates the Hausdorff dimension given by Eq. 2 is $D_H = 1.1$, which is approximately the fractal dimension obtained in the preceding section. The maximum abscissa value of -1.9 corresponds to a cutoff radius of 6.8 Å and the minimum ordinate value of -2.4 corresponds to 11 Å. The points outside this range are not presented in the figure because below 6.8 Å, the jumps shown in Figure 2 lead to discontinuous data, and above 11 Å the system reaches a saturation level¹⁶ and the slope equates to unity.

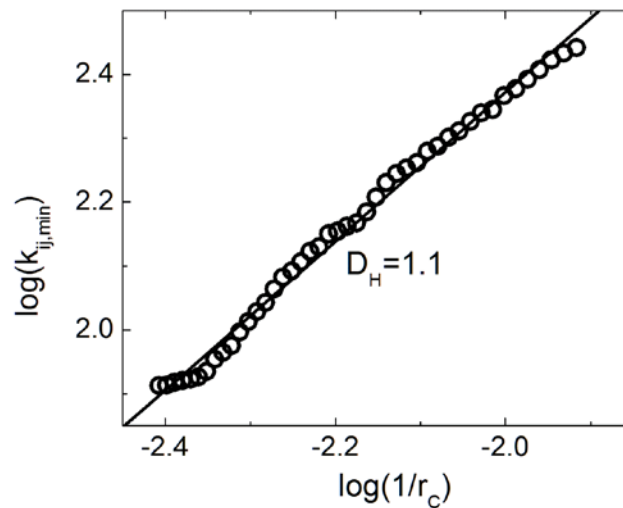


FIG 3. Hausdorff dimension obtained as the average from 150 paths in 10 proteins.

In Figure 4, we present the residues visited during signal propagation for the allosteric shortest path for 1GPW.pdb from residue LYS132 to ASP98. The shortest path with a cutoff radius of 6.9 Å reaches ASP98 in six steps (See Supplementary Material). Abscissa values indicate residues indices and ordinate values show the frequency of visits to the residues while going from the initial point to the final on the path, i.e., in going from LYS132 to ASP98. As the different ordinate values indicate, some residues will be visited more frequently than others. Several paths from LYS132 to ASP98 are possible, but only one set of residues gives the shortest path, shown by the dark circles identified during backtracking. The importance of these residues in allosteric communication for 1GPW.pdb has been shown before^{17,18}. The path residues are situated in the highly visited regions in the figure. The list of residues visited during forward tracking is given in the Supplementary Material Part 2 and the residues on the shortest path, obtained during backtracking are highlighted in that list.

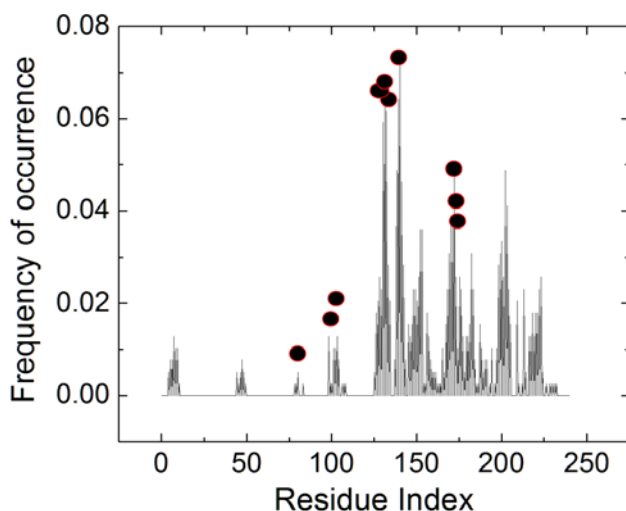


FIG 4. Residues on all paths from LYS132 to ASP98 for 1GPW.pdb. Shortest path residues are indicated by filled circles.

Calculations over 10^5 random paths of six steps, starting from LYS132 and terminating at ASP98 showed that the entropy of the shortest path is larger than 95% of the entropies of the random paths. Thus, in the absence of constraints, signal transport prefers high entropy routes through the protein.

Discussion and Conclusions

We studied fractal dimensions of shortest paths as a function of the interaction cutoff radius. The transition of the fractal dimension from multifractal to self similar regimes takes place at 6.8 Å which equates to the radius of the first coordination shell in the alpha carbon representation of native proteins. The number of steps to go between two points exhibits sharp discontinuities around cutoff lengths of 4 Å. Below 3.8 Å the system is non-percolating, as in the bond percolation problem, and a path between two points does not exist. The fractal dimension of shortest paths at and above the cutoff value of 6.8 Å is $D = 1.12 \pm 0.03$, remarkably close to $D = 1$ of Euclidean dense homogeneous systems where the shortest distance between two points is a straight line. The Hausdorff dimension of shortest paths is 1.1, close to the value obtained by using Eq. 1. In step sizes much less than 6.8 Å information travels in a diffusive manner with higher dimensionalities of paths carrying this information. If the signal were not directional, then it would be equal to 2.5 from the work of Enright and Leitner at the shortest wavelength⁵ instead of 1.4 from Figure 1. Perturbing a residue perturbs, in turn, several residues directly connected to it by the network structure of the protein. Thus the perturbations spread into the protein and a multitude of perturbation pathways of differing lengths, originating from a point and ending at another, becomes possible. We proposed an algorithm to find the residues along the shortest of these paths. Knowledge of the residues along a path may have important ramifications, particularly in understanding and controlling allosteric communication or even non-allosteric signal transport¹⁹. One may make the plausible assumption that allosteric information travels on a shortest path from the effector site to the active site. A detailed study of this conjecture requires optimization of the variables imposed by evolution. An excellent example of constrained optimization to calculate fractal dimensions is by West et al, who calculated the scaling exponents for biological systems that optimize the surface area to volume ratios²⁰. For shortest path scaling, we do not know yet what the constraints for information flow are. However, the present calculations show that shortest path residues lie mostly on high entropy routes. The present calculations also show that entropy of information transport from the effector to active site is not equal to that in the reverse direction, leading to the conclusion that allosteric communication is directional.

The present analysis is based on information from the contact map of proteins with a preselected interaction cutoff radius. The emergence of the cutoff radius approximately as 6.8 Å above which the paths are mono-fractal is not a coincidence. That this value of the cutoff is the value for which the Gaussian Network Model (GNM)²¹ performs best has been shown in a large number of papers. The spectral dimension for slow vibrational modes from GNM with an r_c of 7.0 Å, was shown to be 1.63 in contrast to 3 of the Debye theory³. The relationship between spectral dimension and mass dimension of three dimensional objects, including proteins, has been widely studied. In the present work, we were able to establish an equality of the short path dimensions with Hausdorff dimensions only. Unlike the GNM work, the fractal dimension of 1.1 is structural only and is not a spectral quantity. Spectral dimension of shortest paths, which will be less than or equal to 1.1, should be calculated with a dynamic model of transmission over a path and awaits future work.

The present calculations are based on the alpha carbon coarse grained approximation which should suffice for a proof of principle approach. Although atomic detail should not change the overall picture, specific values may slightly depend on the coarseness of atomic organization as has been shown in the calculations of mass fractal dimensions of proteins⁵.

As a final remark, the present study of signal flow focuses on the structural view of allosteric communication only and does not consider the enthalpic side of the phenomenon. Although a large number of papers show the importance of structure on allosteric transmission^{18, 22-26} the structural versus enthalpic picture has recently been brought into attention by Motlagh et. al.²⁷, which definitely deserves attention. In this respect, the present model is only a partial picture of the complete process of signal transport in proteins.

Acknowledgment: The author gratefully acknowledges fruitful discussions with Professor Ahmet Gul, School of Medicine, Istanbul University.

References

1. D. M. Leitner, *Annual Review of Physical Chemistry*, 2008, **59**, 233-259.
2. D. Benavraham, *Phys Rev B*, 1993, **47**, 14559-14560.
3. T. Haliloglu, I. Bahar and B. Erman, *Physical Review Letters*, 1997, **79**, 3090-3093.
4. R. Burioni, D. Cassi, F. Cecconi and A. Vulpiani, *Proteins*, 2004, **55**, 529-535.
5. M. B. Enright and D. M. Leitner, *Phys Rev E*, 2005, **71**.
6. M. Manhart and A. V. Morozov, *Physical Review Letters*, 2013, **111**.
7. J. Liang and K. A. Dill, *Biophys J*, 2001, **81**, 751-766.
8. J. P. Allen, J. T. Colvin, D. G. Stinson, C. P. Flynn and H. J. Stapleton, *Biophys J*, 1982, **38**, 299-310.
9. J. T. Colvin, G. C. Wagner, J. P. Allen and H. J. Stapleton, *Biophys J*, 1984, **45**, A130-A130.
10. M. de Leeuw, S. Reuveni, J. Klafter and R. Granek, *Plos One*, 2009, **4**.
11. R. Elber and M. Karplus, *Physical Review Letters*, 1986, **56**, 394-397.
12. R. Granek and J. Klafter, *Physical Review Letters*, 2005, **95**.
13. H. J. Stapleton, J. P. Allen, C. P. Flynn, D. G. Stinson and S. R. Kurtz, *Physical Review Letters*, 1980, **45**, 1456-1459.
14. G. C. Wagner, J. T. Colvin, J. P. Allen and H. J. Stapleton, *J Am Chem Soc*, 1985, **107**, 5589-5594.
15. A. R. Atilgan, P. Akan and C. Baysal, *Biophys J*, 2004, **86**, 85-91.
16. W. Kinsner, *ICCI 2005: Fourth IEEE International Conference on Cognitive Informatics - Proceedings*, 2005, 58-72.
17. R. E. Amaro, A. Sethi, R. S. Myers, V. J. Davisson and Z. A. Luthey-Schulten, *Biochemistry-U.S.*, 2007, **46**, 2156-2173.
18. B. Erman, *Proteins*, 2013, **81**, 1097-1101.
19. M. W. Clarkson, S. A. Gilmore, M. H. Edgell and A. L. Lee, *Biochemistry-U.S.*, 2006, **45**, 7693-7699.
20. G. B. West, J. H. Brown and B. J. Enquist, *Science*, 1999, **284**, 1677-1679.
21. C. Tuzmen and B. Erman, *Plos One*, 2011, **6**, e16474.

22. W. A. Eaton, E. R. Henry, J. Hofrichter and A. Mozzarelli, *Nature Structural Biology*, 1999, **6**, 351-358.
23. S. Tang, J. C. Liao, A. R. Dunn, R. B. Altman, J. A. Spudich and J. P. Schmidt, *Journal of Molecular Biology*, 2007, **373**, 1361-1373.
24. A. T. VanWart, J. Eargle, Z. Luthey-Schulten and R. E. Amaro, *J Chem Theory Comput*, 2012, **8**, 2949-2961.
25. S. W. Lockless and R. Ranganathan, *Science*, 1999, **286**, 295-299.
26. B. Erman, *Physical Biology*, 2011, **8**, 056003 (056009pp).
27. H. N. Motlagh, J. O. Wrabl, J. Li and V. J. Hilser, *Nature*, 2014, **508**, 331-339.

SUPPLEMENTARY MATERIAL

1. Derivation of Eq. 1

Taking the logarithm of both sides of the expression $r_{ij}^D = A k_{ij,\min} r_C$ we obtain

$$\log(k_{ij,\min} r_C) = -\log(A) + D \log(r_{ij}) \quad (S1)$$

Taking $\log(k_{ij,\min} r_C)$ as the y-axis and $\log(r_{ij})$ as the x-axis, Eq 1 plots as a straight line with $-\log(A)$ as the y-intercept and D as the slope. The slope is written for points 1 and 2 as

$$D = \frac{\log(k_{ij,\min}(2)r_C) - \log(k_{ij,\min}(1)r_C)}{\log(r_{ij}(2)) - \log(r_{ij}(1))} \quad (S2)$$

Now we choose a path 1 traversed with $k_{ij,\min}(1)$ steps and another path that is traversed with $k_{ij,\min}(1) + 1$. The length of the first and second paths will be $r_{ij}(1)$ and $r_{ij}(1) + \delta r_{ij}$, respectively, with $r_{ij}(1) \gg 1$ and $r_{ij}(1) \gg \delta r_{ij}$ for large r_{ij} we can write

$$\frac{\log(k_{ij,\min}(2)r_C)}{\log(r_{ij}(2))} = \frac{\log((k_{ij,\min}(1) + 1)r_C)}{\log(r_{ij}(1) + \delta r_{ij})} \approx \frac{\log(k_{ij,\min}(1)r_C)}{\log(r_{ij}(1))} = \frac{\log(k_{ij,\min}(2)r_C) - \log(k_{ij,\min}(1)r_C)}{\log(r_{ij}(2)) - \log(r_{ij}(1))} \equiv D \quad (S3)$$

2. Sample Calculations for 1GPW.pdb

List of residues visited during the six steps in going from LYS132 to ASP98 in 1GPW.pdb. At the kth step, the left column in the following list is the residue in step k-1, the second column is the residue in the kth step. The third column shows the number of different ways a path arrives to the shown residue at the kth step. The highlighted residues are the ones obtained during backtracking. For this, we start from residue 98 at step 6 and identify its path neighbor at step 5. Then, proceed to finding the path neighbor at step 4, etc. Backtracking in this way may result in more than one path which is listed at the bottom of this list. Finally, the residues on the shortest path 1 are shown on the protein.

Residue at step k-1	Residue at step k	Number of paths
Step 1		
132	138	1.000000
132	139	1.000000
132	140	1.000000
132	172	1.000000
132	173	1.000000
132	174	1.000000
Step 2		
138	131	5.000000
138	132	6.000000
138	133	2.000000
138	134	2.000000

138	152	3.000000
138	153	3.000000
139	131	5.000000
139	132	6.000000
139	133	2.000000
139	134	2.000000
139	150	2.000000
139	151	2.000000
139	152	3.000000
139	153	3.000000
140	130	3.000000
140	131	5.000000
140	132	6.000000
140	148	1.000000
140	149	1.000000
140	150	2.000000
140	151	2.000000
140	152	3.000000
140	153	3.000000
172	130	3.000000
172	131	5.000000
172	132	6.000000
172	176	3.000000
172	183	1.000000
172	202	1.000000
173	130	3.000000
173	131	5.000000
173	132	6.000000
174	132	6.000000

Step 3

130	140	30.000000
130	141	13.000000
130	145	5.000000
130	170	7.000000
130	171	14.000000
130	172	29.000000
130	173	26.000000
131	138	25.000000
131	139	31.000000
131	140	30.000000
131	141	13.000000
131	171	14.000000
131	172	29.000000
131	173	26.000000
132	138	25.000000
132	139	31.000000
132	140	30.000000
132	172	29.000000
132	173	26.000000
132	174	16.000000
133	137	7.000000
133	138	25.000000

133	139	31.000000
134	138	25.000000
134	139	31.000000
137	133	13.000000
138	131	21.000000
138	132	19.000000
138	133	13.000000
138	134	13.000000
138	152	11.000000
138	153	9.000000
139	131	21.000000
139	132	19.000000
139	133	13.000000
139	134	13.000000
139	150	10.000000
139	151	12.000000
139	152	11.000000
139	153	9.000000
140	130	15.000000
140	131	21.000000
140	132	19.000000
140	148	6.000000
140	149	8.000000
140	150	10.000000
140	151	12.000000
140	152	11.000000
140	153	9.000000
141	130	15.000000
141	131	21.000000
141	145	5.000000
141	146	2.000000
141	147	4.000000
141	148	6.000000
141	149	8.000000
148	140	30.000000
148	141	13.000000
148	142	4.000000
149	140	30.000000
149	141	13.000000
149	142	4.000000
150	139	31.000000
150	140	30.000000
151	139	31.000000
151	140	30.000000
151	156	8.000000
152	138	25.000000
152	139	31.000000
152	140	30.000000
152	156	8.000000
153	138	25.000000
153	139	31.000000
153	140	30.000000

153	157	3.000000
130	128	4.000000
170	129	11.000000
170	130	15.000000
170	198	1.000000
170	199	1.000000
170	200	3.000000
170	201	4.000000
171	129	11.000000
171	130	15.000000
171	131	21.000000
171	200	3.000000
171	201	4.000000
171	202	10.000000
172	130	15.000000
172	131	21.000000
172	132	19.000000
172	176	10.000000
172	183	5.000000
172	202	10.000000
173	130	15.000000
173	131	21.000000
173	132	19.000000
174	132	19.000000
175	182	5.000000
175	183	5.000000
175	202	10.000000
175	203	7.000000
176	172	29.000000
176	202	10.000000
176	203	7.000000
183	172	29.000000
183	175	11.000000
183	187	1.000000
202	171	14.000000
202	172	29.000000
202	175	11.000000
202	176	10.000000
202	177	7.000000
202	182	5.000000
202	223	1.000000

Step 4

128	101	4.000000
128	102	4.000000
128	103	15.000000
128	168	16.000000
128	169	42.000000
128	170	86.000000
129	103	15.000000
129	169	42.000000
129	170	86.000000
129	171	129.000000

130	140	155.000000
130	141	126.000000
130	145	38.000000
130	170	86.000000
130	171	129.000000
130	172	154.000000
130	173	135.000000
131	138	124.000000
131	139	183.000000
131	140	155.000000
131	141	126.000000
131	171	129.000000
131	172	154.000000
131	173	135.000000
132	138	124.000000
132	139	183.000000
132	140	155.000000
132	172	154.000000
132	173	135.000000
132	174	95.000000
133	137	94.000000
133	138	124.000000
133	139	183.000000
134	138	124.000000
134	139	183.000000
137	133	107.000000
138	131	213.000000
138	132	204.000000
138	133	107.000000
138	134	107.000000
138	152	137.000000
138	153	132.000000
139	131	213.000000
139	132	204.000000
139	133	107.000000
139	134	107.000000
139	150	98.000000
139	151	107.000000
139	152	137.000000
139	153	132.000000
140	130	160.000000
140	131	213.000000
140	132	204.000000
140	148	69.000000
140	149	79.000000
140	150	98.000000
140	151	107.000000
140	152	137.000000
140	153	132.000000
141	130	160.000000
141	131	213.000000
141	145	38.000000

141	146	26.000000
141	147	38.000000
141	148	69.000000
141	149	79.000000
142	104	4.000000
142	146	26.000000
142	147	38.000000
142	148	69.000000
142	149	79.000000
145	130	160.000000
145	141	126.000000
146	141	126.000000
146	142	38.000000
147	141	126.000000
147	142	38.000000
147	143	15.000000
148	140	155.000000
148	141	126.000000
148	142	38.000000
149	140	155.000000
149	141	126.000000
149	142	38.000000
150	139	183.000000
150	140	155.000000
151	139	183.000000
151	140	155.000000
151	156	47.000000
152	138	124.000000
152	139	183.000000
152	140	155.000000
152	156	47.000000
153	138	124.000000
153	139	183.000000
153	140	155.000000
153	157	29.000000
154	158	23.000000
155	159	17.000000
156	151	107.000000
156	152	137.000000
156	160	11.000000
157	153	132.000000
157	161	3.000000
157	194	3.000000
168	126	8.000000
168	127	19.000000
168	128	37.000000
168	197	3.000000
168	198	15.000000
168	199	19.000000
169	126	8.000000
169	127	19.000000
169	128	37.000000

169	129	64.000000
169	198	15.000000
169	199	19.000000
169	200	30.000000
170	128	37.000000
170	129	64.000000
170	130	160.000000
170	198	15.000000
170	199	19.000000
170	200	30.000000
170	201	36.000000
171	129	64.000000
171	130	160.000000
171	131	213.000000
171	200	30.000000
171	201	36.000000
171	202	89.000000
172	130	160.000000
172	131	213.000000
172	132	204.000000
172	176	112.000000
172	183	50.000000
172	202	89.000000
173	130	160.000000
173	131	213.000000
173	132	204.000000
174	132	204.000000
175	182	36.000000
175	183	50.000000
175	202	89.000000
175	203	51.000000
176	172	154.000000
176	202	89.000000
176	203	51.000000
177	202	89.000000
177	203	51.000000
178	203	51.000000
181	203	51.000000
181	204	24.000000
181	205	9.000000
181	209	7.000000
182	175	121.000000
182	202	89.000000
182	203	51.000000
182	204	24.000000
182	209	7.000000
182	213	9.000000
183	172	154.000000
183	175	121.000000
183	187	8.000000
184	188	4.000000
184	213	9.000000

184	216	2.000000
185	189	3.000000
186	190	2.000000
187	183	50.000000
187	191	1.000000
187	216	2.000000
187	217	1.000000
198	167	5.000000
198	168	16.000000
198	169	42.000000
198	170	86.000000
198	218	5.000000
198	219	2.000000
198	220	5.000000
199	168	16.000000
199	169	42.000000
199	170	86.000000
199	218	5.000000
199	219	2.000000
199	220	5.000000
199	221	9.000000
199	222	9.000000
200	169	42.000000
200	170	86.000000
200	171	129.000000
200	213	9.000000
200	218	5.000000
200	220	5.000000
200	221	9.000000
200	222	9.000000
201	170	86.000000
201	171	129.000000
201	221	9.000000
201	222	9.000000
201	223	15.000000
202	171	129.000000
202	172	154.000000
202	175	121.000000
202	176	112.000000
202	177	44.000000
202	182	36.000000
202	223	15.000000
203	175	121.000000
203	176	112.000000
203	177	44.000000
203	178	35.000000
203	179	22.000000
203	180	15.000000
203	181	18.000000
203	182	36.000000
204	179	22.000000
204	180	15.000000

204	181	18.000000
204	182	36.000000
204	209	7.000000
204	223	15.000000
223	7	1.000000
223	8	1.000000
223	9	1.000000
223	201	36.000000
223	202	89.000000
223	204	24.000000

Step 5

7	44	2.000000
7	45	1.000000
7	46	2.000000
7	47	3.000000
7	220	90.000000
7	221	115.000000
7	222	117.000000
7	223	173.000000
8	44	2.000000
8	46	2.000000
8	47	3.000000
8	48	2.000000
8	222	117.000000
8	223	173.000000
8	224	19.000000
9	47	3.000000
9	48	2.000000
9	49	1.000000
9	222	117.000000
9	223	173.000000
9	224	19.000000
101	78	4.000000
101	79	4.000000
101	80	8.000000
101	125	36.000000
101	126	127.000000
101	127	195.000000
101	128	418.000000
102	80	8.000000
102	83	4.000000
102	106	23.000000
102	126	127.000000
102	127	195.000000
102	128	418.000000
103	107	19.000000
103	127	195.000000
103	128	418.000000
103	129	701.000000
104	108	4.000000
104	142	406.000000
104	143	155.000000

126	99	12.000000
126	100	16.000000
126	101	68.000000
126	102	87.000000
126	165	46.000000
126	166	14.000000
126	167	104.000000
126	168	234.000000
126	169	428.000000
127	101	68.000000
127	102	87.000000
127	103	128.000000
127	165	46.000000
127	167	104.000000
127	168	234.000000
127	169	428.000000
128	101	68.000000
128	102	87.000000
128	103	128.000000
128	168	234.000000
128	169	428.000000
128	170	702.000000
129	103	128.000000
129	169	428.000000
129	170	702.000000
129	171	1009.000000
130	140	1508.000000
130	141	999.000000
130	145	414.000000
130	170	702.000000
130	171	1009.000000
130	172	1394.000000
130	173	1188.000000
131	138	1177.000000
131	139	1604.000000
131	140	1508.000000
131	141	999.000000
131	171	1009.000000
131	172	1394.000000
131	173	1188.000000
132	138	1177.000000
132	139	1604.000000
132	140	1508.000000
132	172	1394.000000
132	173	1188.000000
132	174	726.000000
133	137	599.000000
133	138	1177.000000
133	139	1604.000000
134	138	1177.000000
134	139	1604.000000
137	133	790.000000

138	131	1434.000000
138	132	1273.000000
138	133	790.000000
138	134	790.000000
138	152	920.000000
138	153	856.000000
139	131	1434.000000
139	132	1273.000000
139	133	790.000000
139	134	790.000000
139	150	730.000000
139	151	831.000000
139	152	920.000000
139	153	856.000000
140	130	1137.000000
140	131	1434.000000
140	132	1273.000000
140	148	534.000000
140	149	631.000000
140	150	730.000000
140	151	831.000000
140	152	920.000000
140	153	856.000000
141	130	1137.000000
141	131	1434.000000
141	145	414.000000
141	146	266.000000
141	147	391.000000
141	148	534.000000
141	149	631.000000
142	104	72.000000
142	146	266.000000
142	147	391.000000
142	148	534.000000
142	149	631.000000
143	104	72.000000
143	147	391.000000
145	130	1137.000000
145	141	999.000000
146	141	999.000000
146	142	406.000000
147	141	999.000000
147	142	406.000000
147	143	155.000000
148	140	1508.000000
148	141	999.000000
148	142	406.000000
149	140	1508.000000
149	141	999.000000
149	142	406.000000
150	139	1604.000000
150	140	1508.000000

151	139	1604.000000
151	140	1508.000000
151	156	530.000000
152	138	1177.000000
152	139	1604.000000
152	140	1508.000000
152	156	530.000000
153	138	1177.000000
153	139	1604.000000
153	140	1508.000000
153	157	310.000000
154	158	184.000000
155	159	150.000000
156	151	831.000000
156	152	920.000000
156	160	119.000000
157	153	856.000000
157	161	80.000000
157	194	56.000000
158	154	405.000000
158	162	54.000000
158	193	29.000000
158	194	56.000000
159	155	422.000000
159	163	31.000000
160	156	530.000000
160	164	14.000000
160	165	46.000000
161	157	310.000000
161	165	46.000000
167	125	36.000000
167	126	127.000000
167	127	195.000000
167	196	26.000000
167	197	58.000000
167	198	214.000000
168	126	127.000000
168	127	195.000000
168	128	418.000000
168	197	58.000000
168	198	214.000000
168	199	258.000000
169	126	127.000000
169	127	195.000000
169	128	418.000000
169	129	701.000000
169	198	214.000000
169	199	258.000000
169	200	364.000000
170	128	418.000000
170	129	701.000000
170	130	1137.000000

170	198	214.000000
170	199	258.000000
170	200	364.000000
170	201	386.000000
171	129	701.000000
171	130	1137.000000
171	131	1434.000000
171	200	364.000000
171	201	386.000000
171	202	722.000000
172	130	1137.000000
172	131	1434.000000
172	132	1273.000000
172	176	724.000000
172	183	366.000000
172	202	722.000000
173	130	1137.000000
173	131	1434.000000
173	132	1273.000000
174	132	1273.000000
175	182	382.000000
175	183	366.000000
175	202	722.000000
175	203	525.000000
176	172	1394.000000
176	202	722.000000
176	203	525.000000
177	202	722.000000
177	203	525.000000
178	203	525.000000
179	203	525.000000
179	204	263.000000
179	205	139.000000
180	203	525.000000
180	204	263.000000
180	205	139.000000
181	203	525.000000
181	204	263.000000
181	205	139.000000
181	209	97.000000
182	175	801.000000
182	202	722.000000
182	203	525.000000
182	204	263.000000
182	209	97.000000
182	213	94.000000
183	172	1394.000000
183	175	801.000000
183	187	92.000000
184	188	46.000000
184	213	94.000000
184	216	40.000000

185	189	31.000000
186	190	27.000000
187	183	366.000000
187	191	21.000000
187	216	40.000000
187	217	31.000000
188	184	125.000000
188	216	40.000000
188	217	31.000000
189	185	86.000000
190	186	88.000000
190	194	56.000000
191	187	92.000000
191	217	31.000000
194	157	310.000000
194	158	184.000000
194	190	27.000000
196	166	14.000000
196	167	104.000000
197	167	104.000000
197	168	234.000000
197	219	48.000000
198	167	104.000000
198	168	234.000000
198	169	428.000000
198	170	702.000000
198	218	83.000000
198	219	48.000000
198	220	90.000000
199	168	234.000000
199	169	428.000000
199	170	702.000000
199	218	83.000000
199	219	48.000000
199	220	90.000000
199	221	115.000000
199	222	117.000000
200	169	428.000000
200	170	702.000000
200	171	1009.000000
200	213	94.000000
200	218	83.000000
200	220	90.000000
200	221	115.000000
200	222	117.000000
201	170	702.000000
201	171	1009.000000
201	221	115.000000
201	222	117.000000
201	223	173.000000
202	171	1009.000000
202	172	1394.000000

202	175	801.000000
202	176	724.000000
202	177	430.000000
202	182	382.000000
202	223	173.000000
203	175	801.000000
203	176	724.000000
203	177	430.000000
203	178	365.000000
203	179	196.000000
203	180	159.000000
203	181	214.000000
203	182	382.000000
204	179	196.000000
204	180	159.000000
204	181	214.000000
204	182	382.000000
204	209	97.000000
204	223	173.000000
205	179	196.000000
205	180	159.000000
205	181	214.000000
205	209	97.000000
205	226	26.000000
209	181	214.000000
209	182	382.000000
209	204	263.000000
209	205	139.000000
209	213	94.000000
213	182	382.000000
213	184	125.000000
213	200	364.000000
213	209	97.000000
213	217	31.000000
213	218	83.000000
216	184	125.000000
216	187	92.000000
216	188	46.000000
216	212	18.000000
217	187	92.000000
217	188	46.000000
217	191	21.000000
217	213	94.000000
218	198	214.000000
218	199	258.000000
218	200	364.000000
218	213	94.000000
218	214	19.000000
219	4	7.000000
219	5	17.000000
219	197	58.000000
219	198	214.000000

219	199	258.000000
219	214	19.000000
220	4	7.000000
220	5	17.000000
220	6	24.000000
220	7	40.000000
220	198	214.000000
220	199	258.000000
220	200	364.000000
221	5	17.000000
221	6	24.000000
221	7	40.000000
221	199	258.000000
221	200	364.000000
221	201	386.000000
221	210	25.000000
222	6	24.000000
222	7	40.000000
222	8	27.000000
222	9	27.000000
222	199	258.000000
222	200	364.000000
222	201	386.000000
223	7	40.000000
223	8	27.000000
223	9	27.000000
223	201	386.000000
223	202	722.000000
223	204	263.000000
224	8	27.000000
224	9	27.000000
224	10	3.000000
224	228	3.000000
225	229	2.000000
226	205	139.000000
226	230	1.000000
226	231	1.000000
226	232	1.000000

Step 6

76	98	5.000000
77	98	27.000000
78	98	114.000000
93	98	12.000000
124	98	191.000000

Shortest Path Residues:

Path 1: 132, 173, 130, 128, 101, 78, 98

Path 2: 132, 172, 130, 128, 101, 78, 98

Path 3: 132, 140, 130, 128, 101, 78, 98

3. Residues of Shortest Path 1:

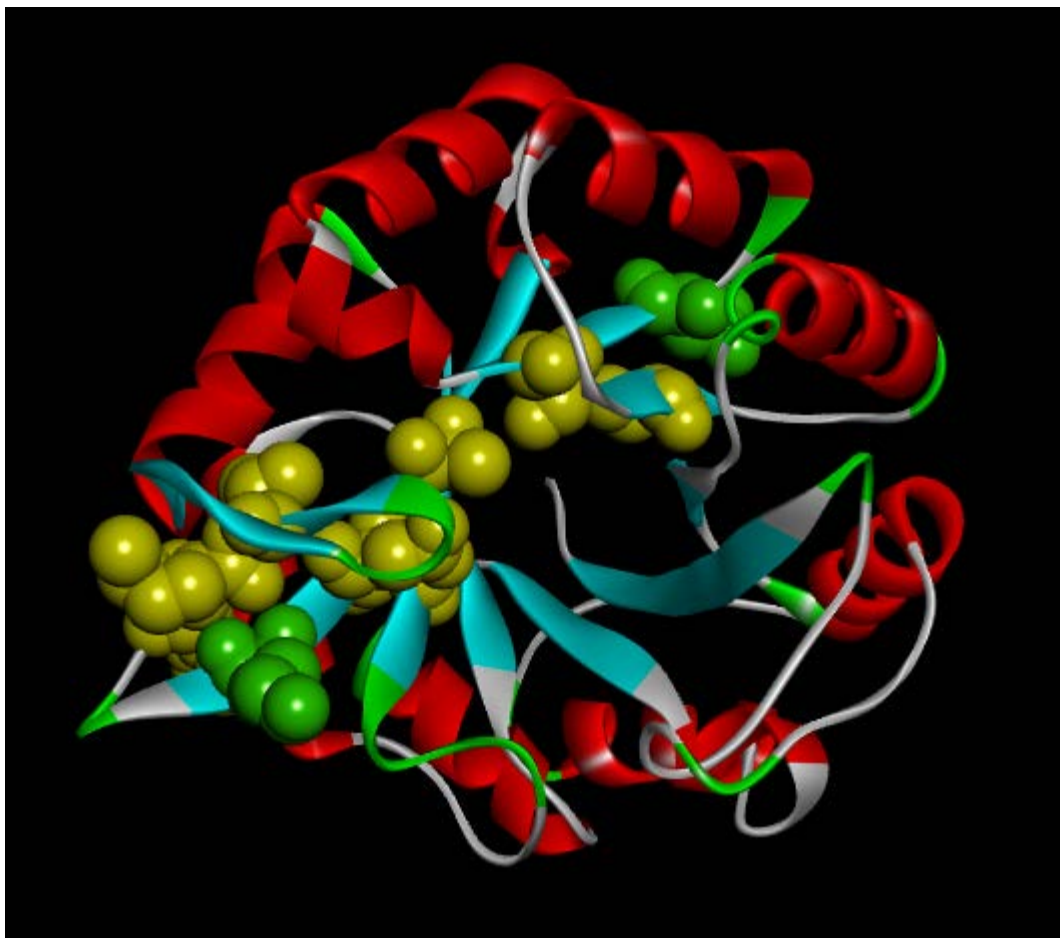


Figure S1. Shortest path residues highlighted in yellow. Terminal residues are in green.